

Effect of Locked-Modes on Impurity Spreading in MHD Simulations of Massive Gas Injection

V.A Izzo

Theory and Simulations of Disruptions Workshop
Princeton, NJ
20 July 2016

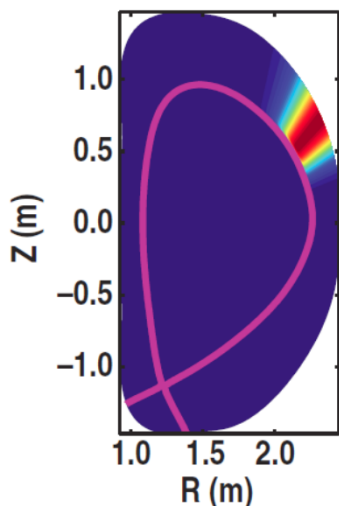
Motivation

- Disruption mitigation is ITER will be applied as a last resort when a disruption is imminent and cannot be avoided by passive or active control
- NTMs leading to locked-modes were found to be the most common root cause of disruptions in JET* (with other root causes also sometimes leading to mode-locking)
- We can assume that disruption mitigation will very frequently be employed when large/locked islands are already present in the plasma
- Disruption mitigation studies with pre-existing islands/locked-modes, using both massive gas injection (MGI) and shattered pellet injection, are part of a 2016 experimental Joint Research Target

NIMROD extended MHD code is combined with KPRAD atomic physics code to model massive gas injection (MGI)

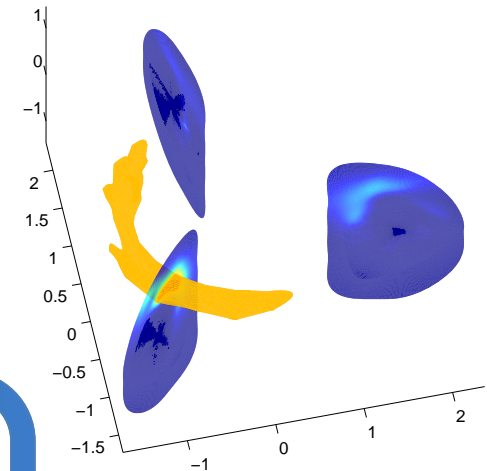
Beginning with DIII-D equilibrium, impurities are deposited as neutrals

Neutral Ne density



KPRAD calculates ionization, recombination and radiation cooling

Ionized Ne density



NIMROD calculates MHD response to edge cooling, diffuses and advects impurities along with main ion species

Outline

Part 1: The physics of impurity plume expansion during massive gas injection (MGI)

Part 2: Results of MGI simulations with pre-existing islands

- Comparison of 2/1 islands with different phases and amplitudes
- The role of the $n=2$ mode
- Simulation with pre-imposed 4/2 island

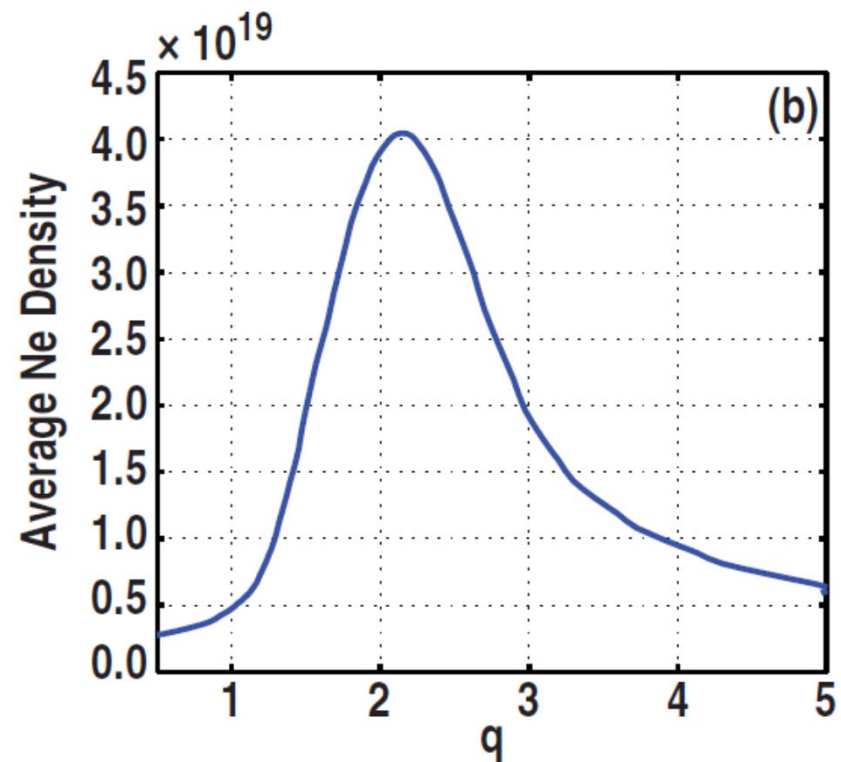
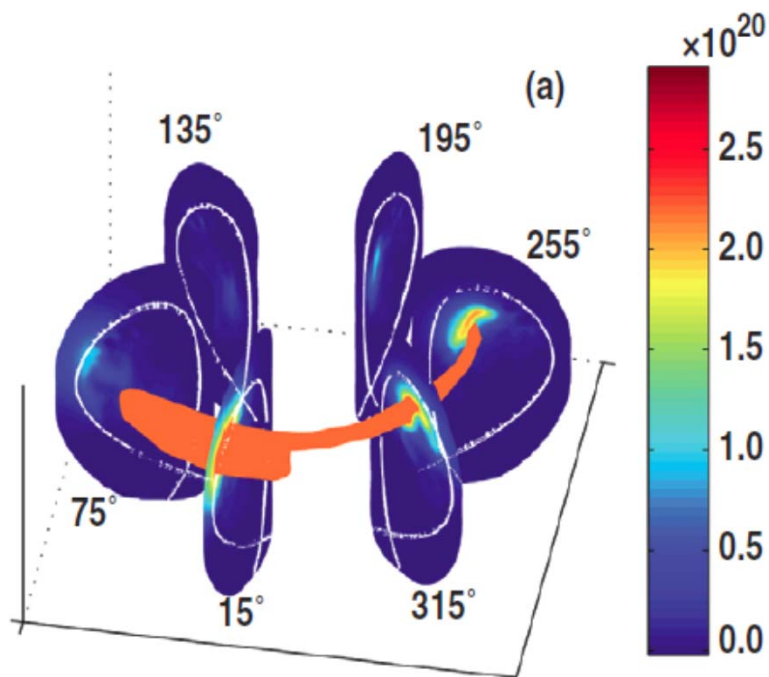
Part 3: Consequences for radiated energy fraction and toroidal peaking factor

PART 1: The physics of impurity plume expansion during massive gas injection (MGI)

Impurities spread along field lines fastest at the $q=2$ surface AND toward the high-field side

→ Impurities spread along field lines fastest at the $q=2$ surface AND toward the high-field side

→ Impurities spread along field lines fastest at the $q=2$ surface AND toward the high-field side



Expansion is also toroidally asymmetric due to magnetic field gradient

Nozzle equation explains preferential HFS spreading:

Continuity $\rho A U = \text{constant}$

$$BA = \text{constant} \Rightarrow \frac{d\rho}{\rho} + \frac{dU}{U} - \frac{dB}{B} = 0$$

Momentum $\rho U dU = -dp = -(dp / d\rho) d\rho = -C_s^2 d\rho$

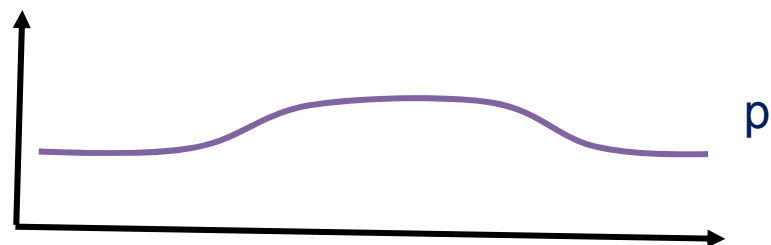
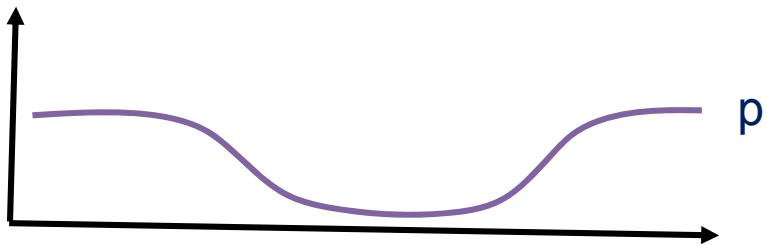
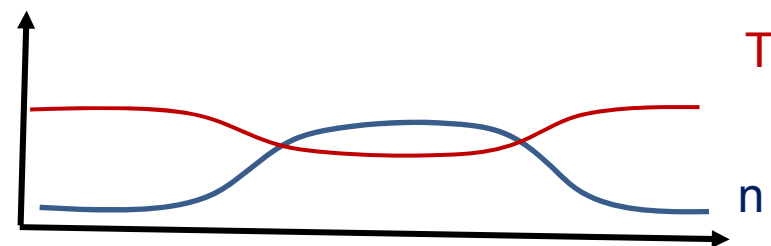
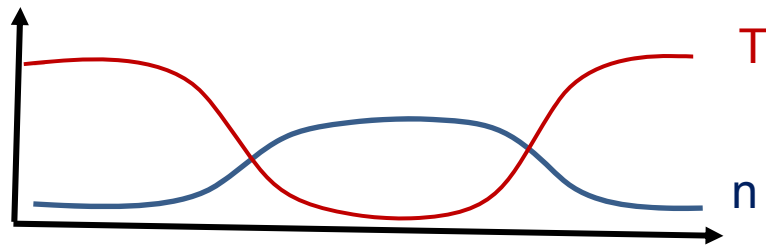
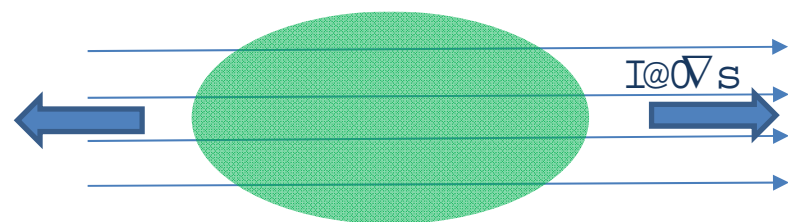
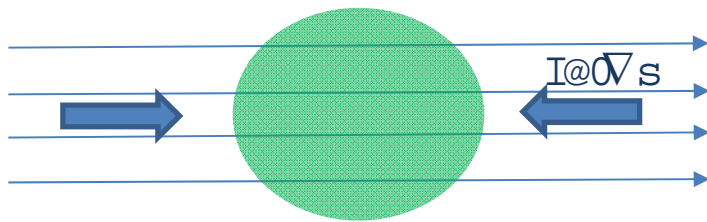
$$\Rightarrow \frac{dU}{U} = \frac{1}{(1-M^2)} \frac{dB}{B}$$

Flow starts at $M < 1$, is thwarted where $dB/B < 0$, accelerates where $dB/B > 0$

Parallel spreading is driven by parallel heat transport

H{foxglj#khd#wdqvsru#Wk#shvxun#bWk#
 arfd}hg#p sxu#w#are#rxog#eh#rzh#wkd#wk#
 vxurxoglj#solv p d

Südoñk#hp d#htx#beüw#r#urgxfhv#ö#
 shvxun#judghqw#sursru#w#rd#r#wk#hghq#w#
 judghqw#k#fk#guy#hv#h#{sdqv#r#xw#dug



Thermal equilibration happens faster at a low order rational surface

Diagram illustrating thermal equilibration at a low-order rational surface. A green oval represents the surface, and blue arrows indicate the direction of particle flow. The diagram shows a single loop of particle flow around the surface.

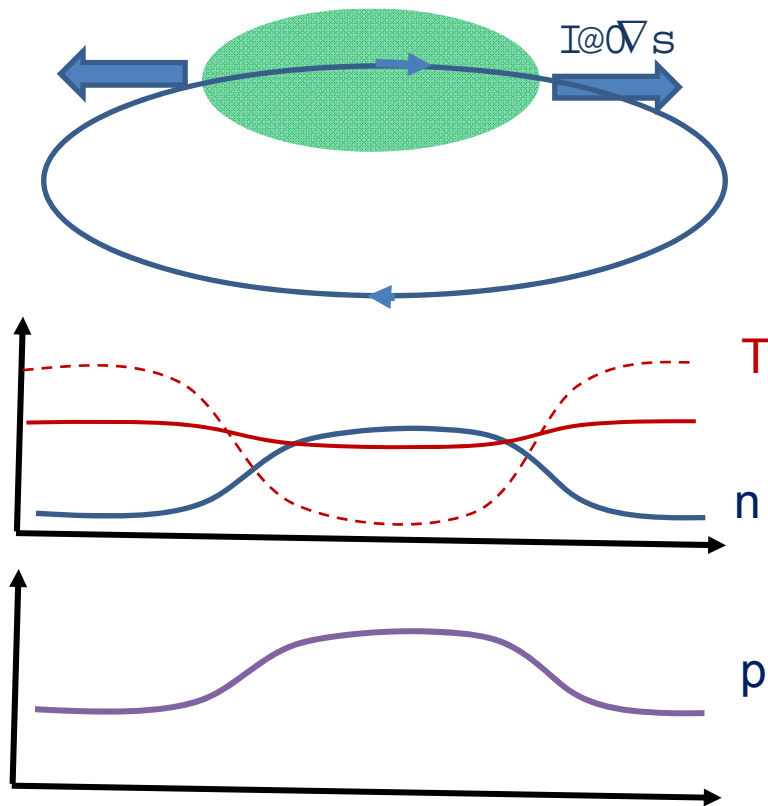
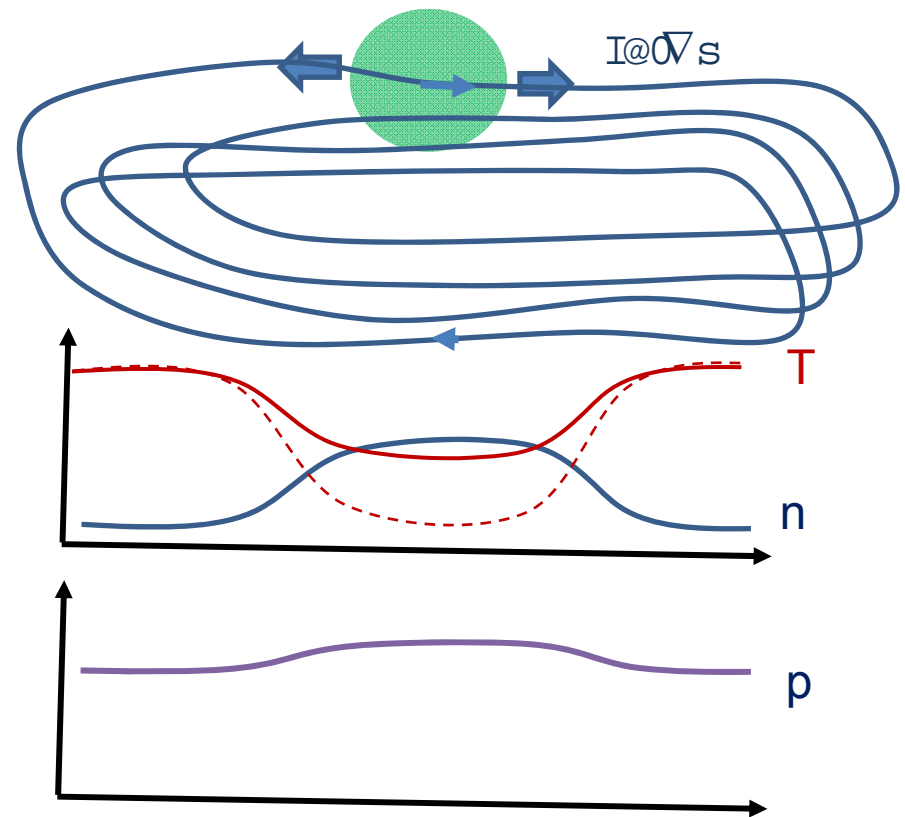


Diagram illustrating thermal equilibration at a high-order rational surface. A green circle represents the surface, and blue arrows indicate the direction of particle flow. The diagram shows multiple loops of particle flow around the surface.



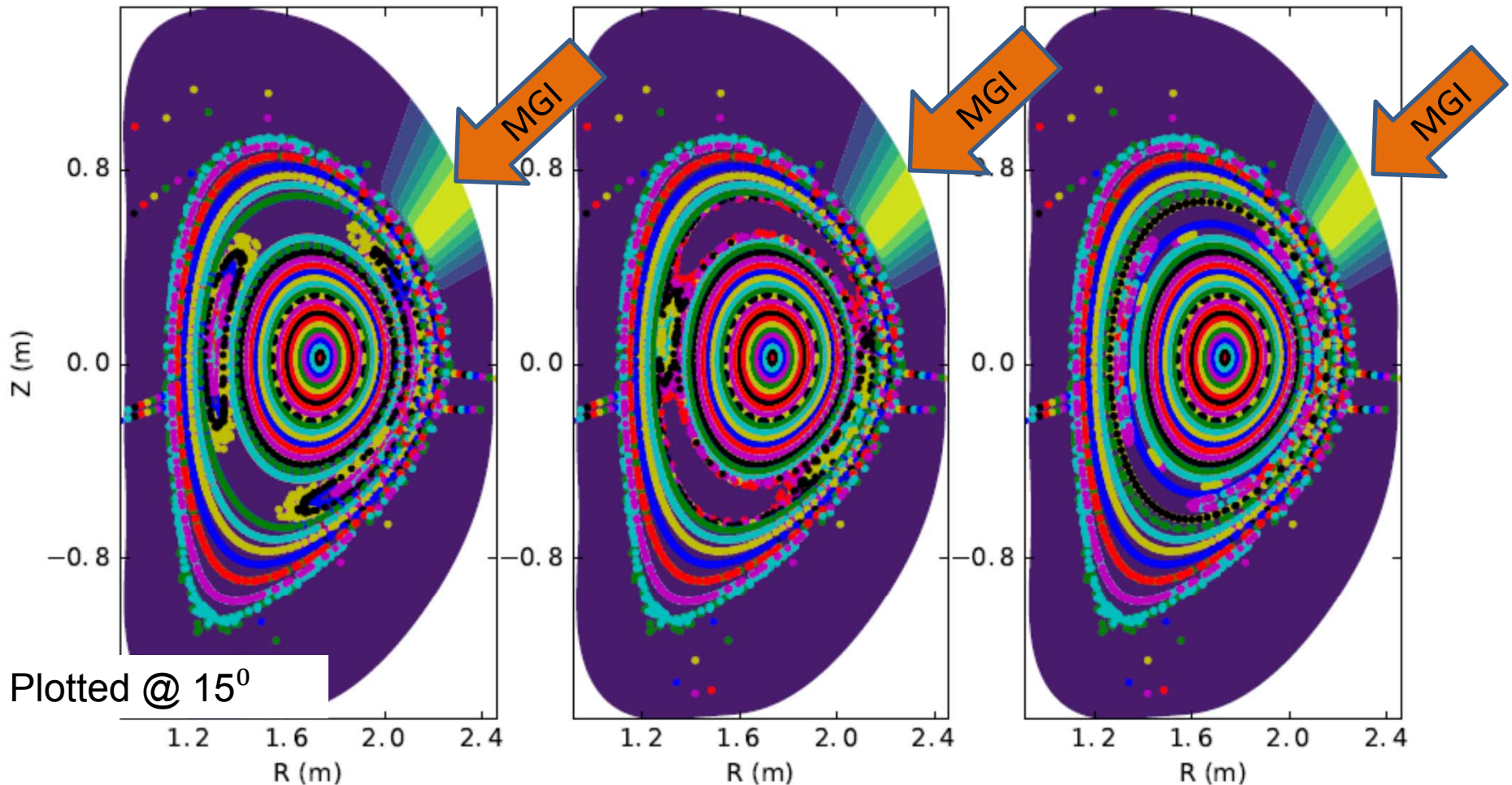
PART 2: Results of MGI simulations with pre-existing islands

Three simulations are initialized with 2/1 magnetic islands

0-phase, large island

180-phase, large island

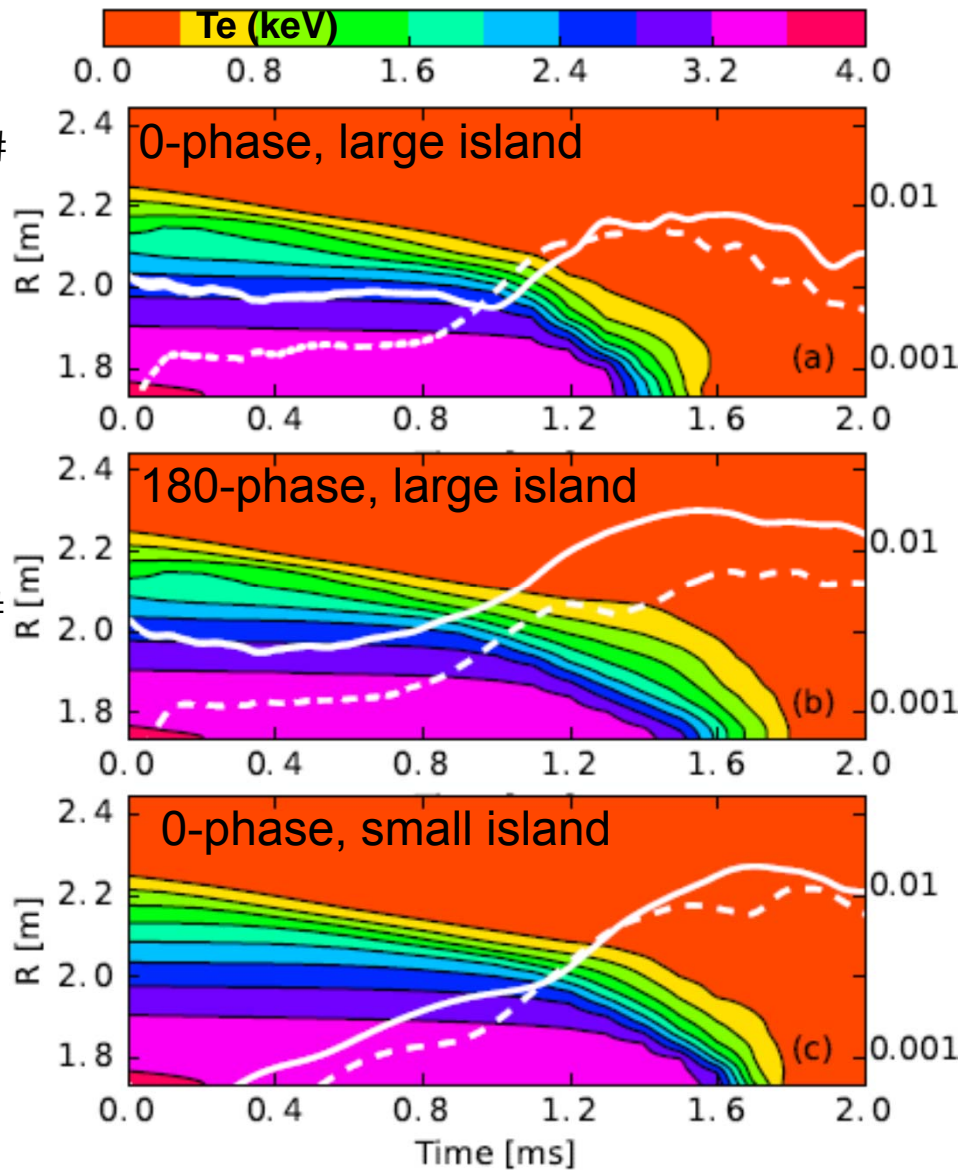
0-phase, small island



MGI location is not aligned precisely with the x-point or the o-point for either phase

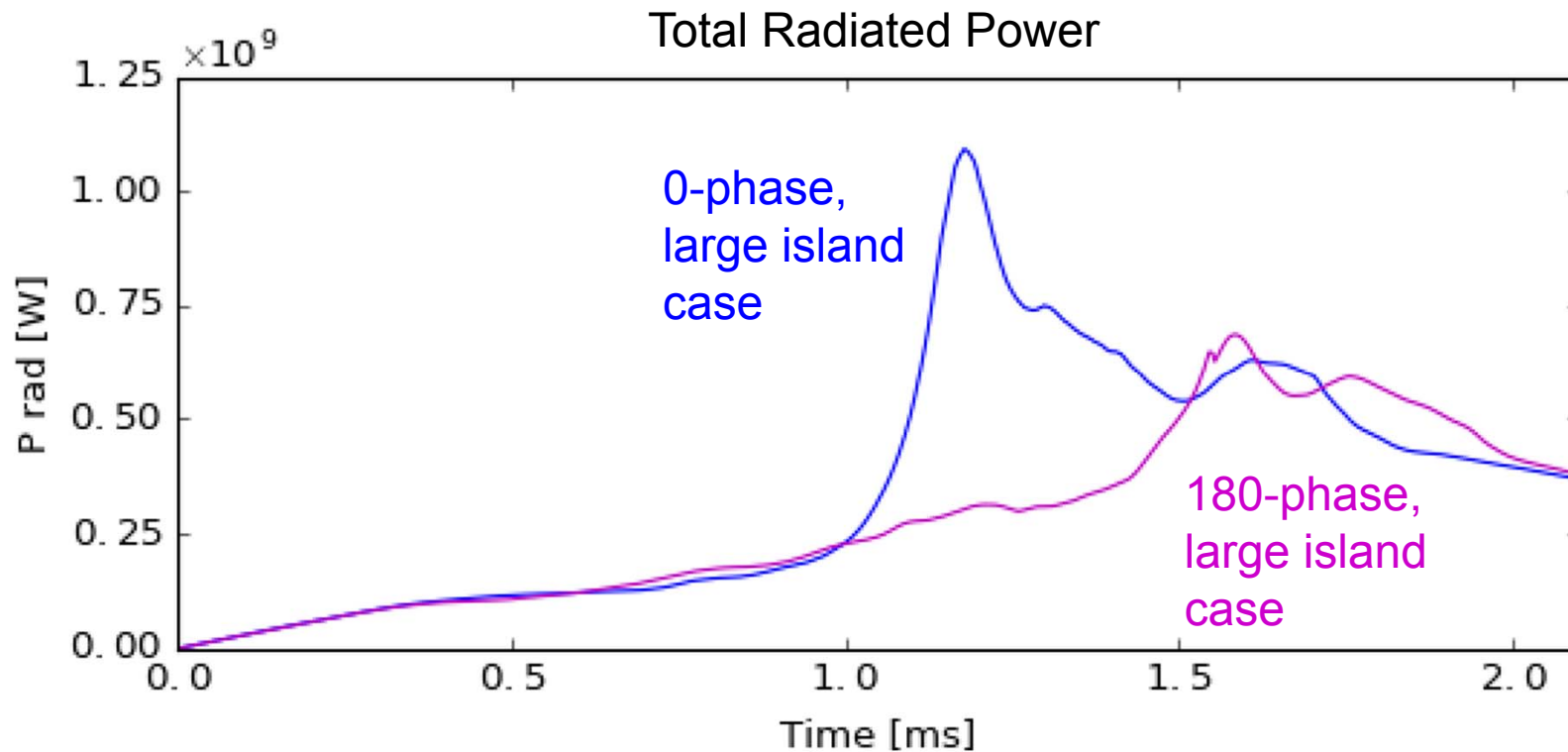
TQ onset time, duration related to initial island width, phase respectively

- From xu#ri#h#yv#
w#h#d#g#d#m#d#g#k#v#
-#x#w#p#b#s#d#h#
- I#o#w#h#q#b#j#e#x#h#r#
b#l#w#d#5#24#l#v#o#l#g#
d#s#s#d#h#q#w#l#b#l#u#j#h#
l#v#o#l#g#f#d#v#h#
- G#u#r#s#l#q#f#h#o#w#d#h#
e#h#j#b#v#h#w#e#h#i#r#h#15#
p#v#z#2#l#u#j#h#l#v#o#l#g#/
o#w#h#z#w#k#p#d#l#v#o#l#g#
- G#x#u#w#i#r#q#i#h#T#h#r#q#j#h#
i#r#h#;3#s#k#d#v#h#w#k#d#g#
h#w#h#u#f#d#v#h#z#w#k#0#
s#k#d#v#h#



- Z#k#w#h#b#h#v#h#h#4#
-#v#r#g#d#g#h#5#
-#g#d#v#k#h#g#h#l#p#s#d#w#g#h#v#
-#l#b#k#q#w#h#i#h#E2E#
- I#o#h#w#h#u#h#0#s#k#d#v#h#
f#d#v#h#w#h#h#q#5#
d#p#s#d#w#g#h#h#f#h#h#g#v#
w#h#h#4#l#p#s#d#w#g#h#r#u#
d#e#u#h#h#l#w#h#y#d#
d#u#r#x#g#w#h#w#d#w#h#
w#h#h#T#
- I#o#h#;3#0#s#k#d#v#h#f#d#v#h#
w#h#h#4#l#p#r#g#h#h#
d#z#d#l#v#g#r#p#l#q#w#

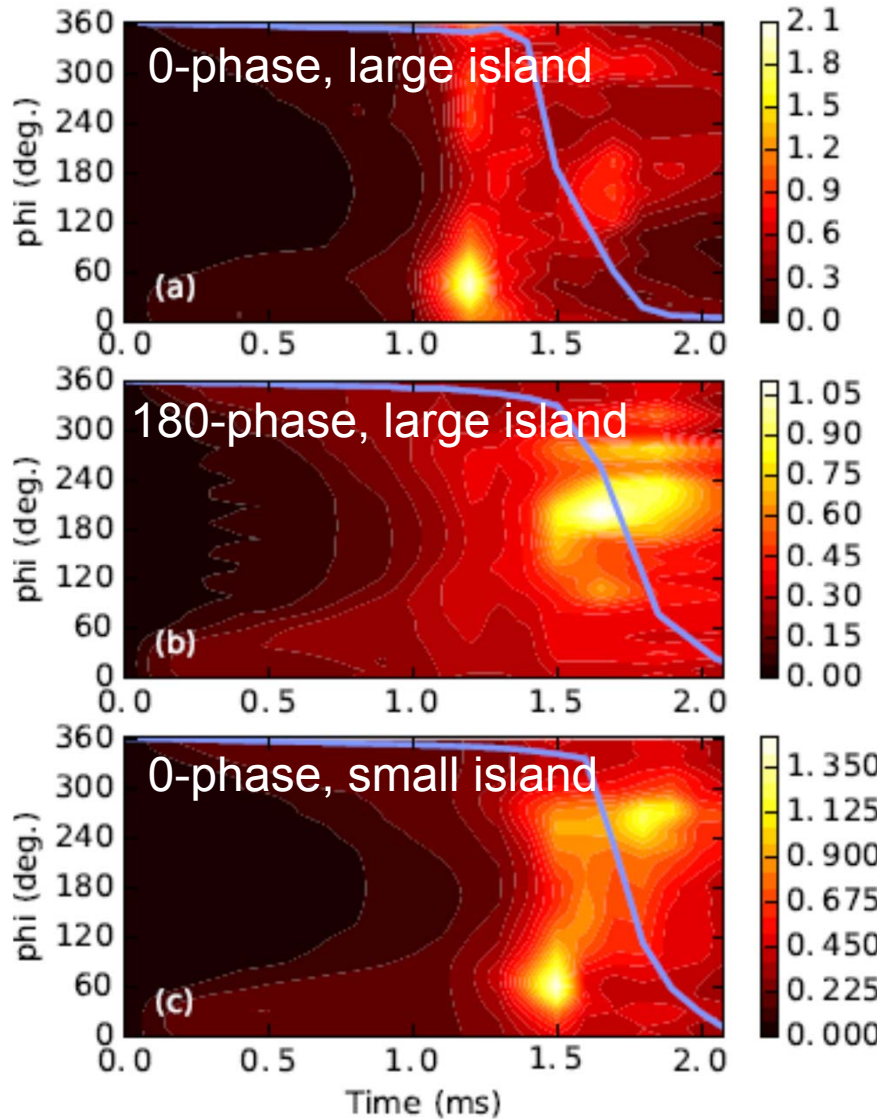
Peak in radiated power is later for 180-phase with same size island



At 0-phase, large initial flash in radiated power appears that is almost completely absent for 180-phase island

Two radiation flashes in each case; difference in relative amplitude

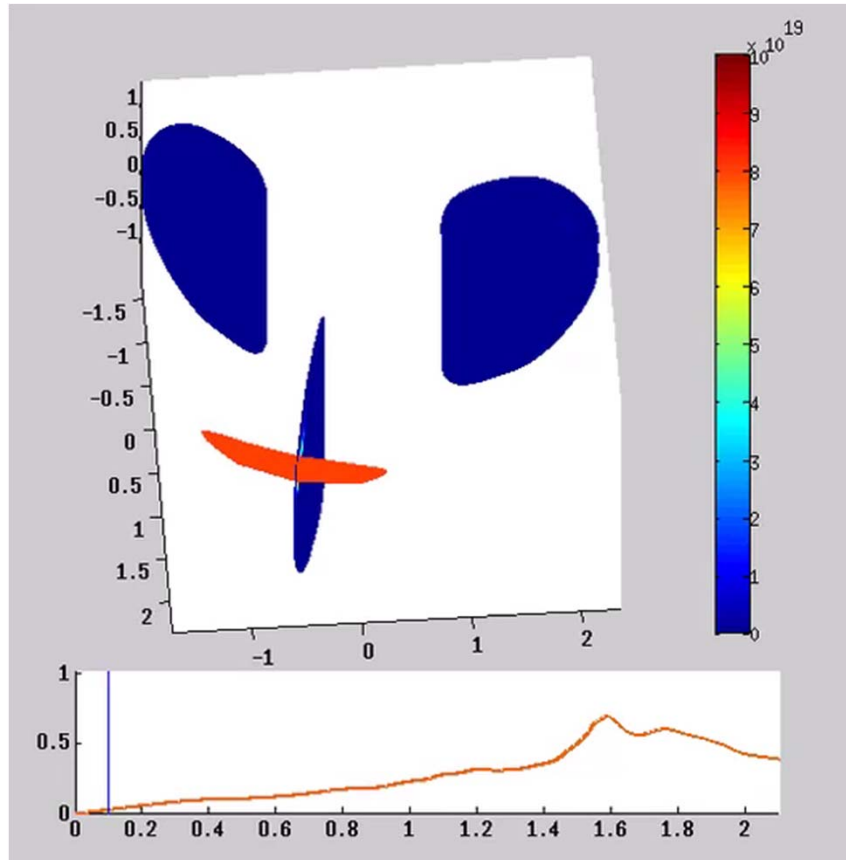
- From $x_{u, r} = S_{u, g} y_{u, r}$ with $\theta = 48^\circ$,
- $S_{u, g} = \begin{pmatrix} 1 & 0 \\ 0 & 1 \end{pmatrix}$ for $\theta = 0^\circ$, $S_{u, g} = \begin{pmatrix} \cos \theta & \sin \theta \\ -\sin \theta & \cos \theta \end{pmatrix}$ for $\theta = 180^\circ$
- Hydrodynamic simulation results



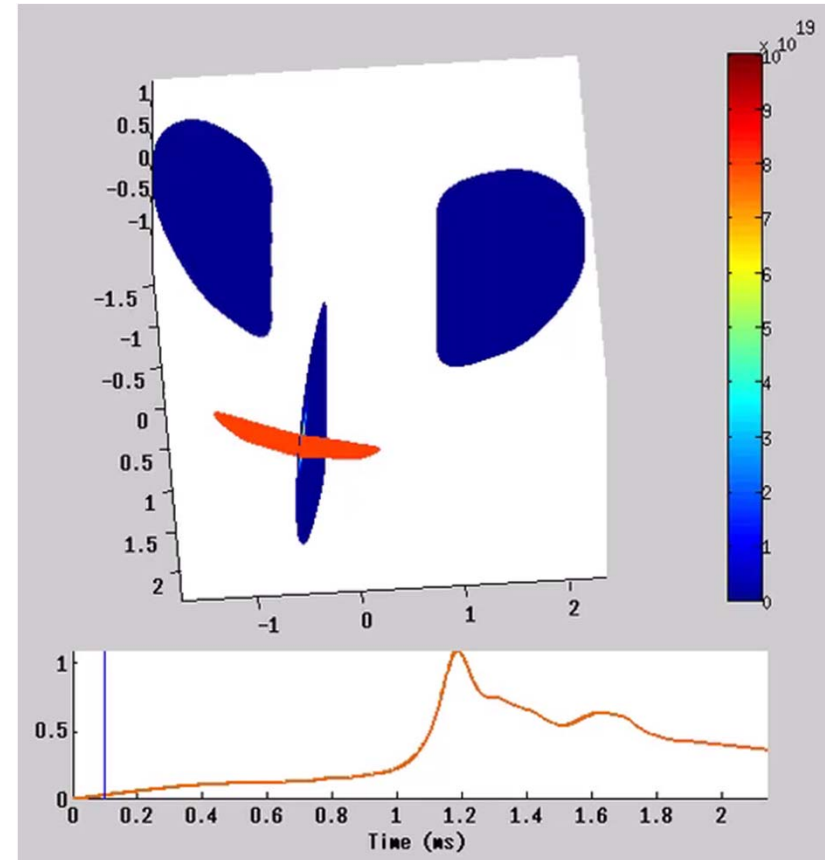
- Simulation results for different island sizes and phases.
- Comparison of radiation flash characteristics.

After 1 ms, parallel spreading differs between the two phases

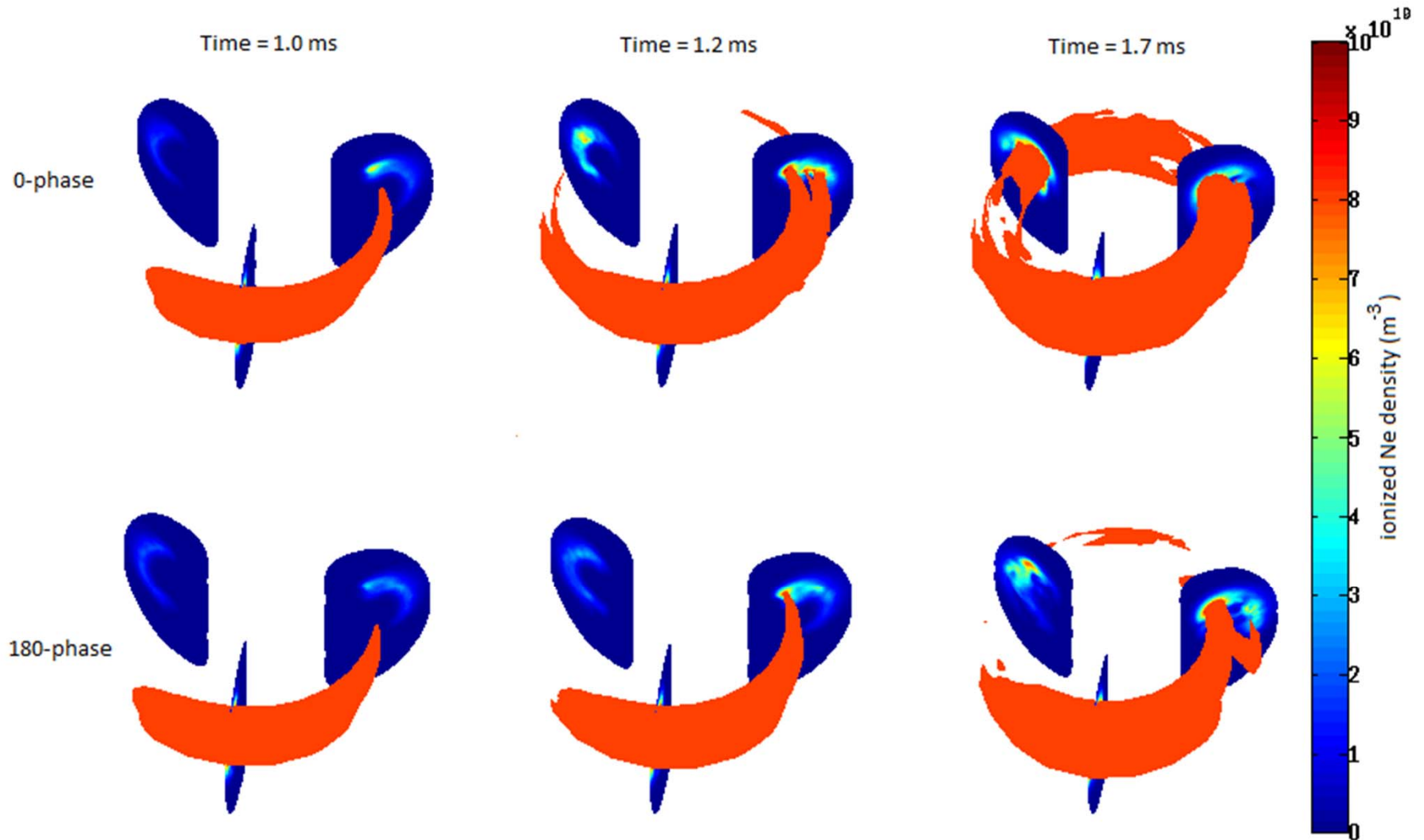
180-phase, large island



0-phase, large island

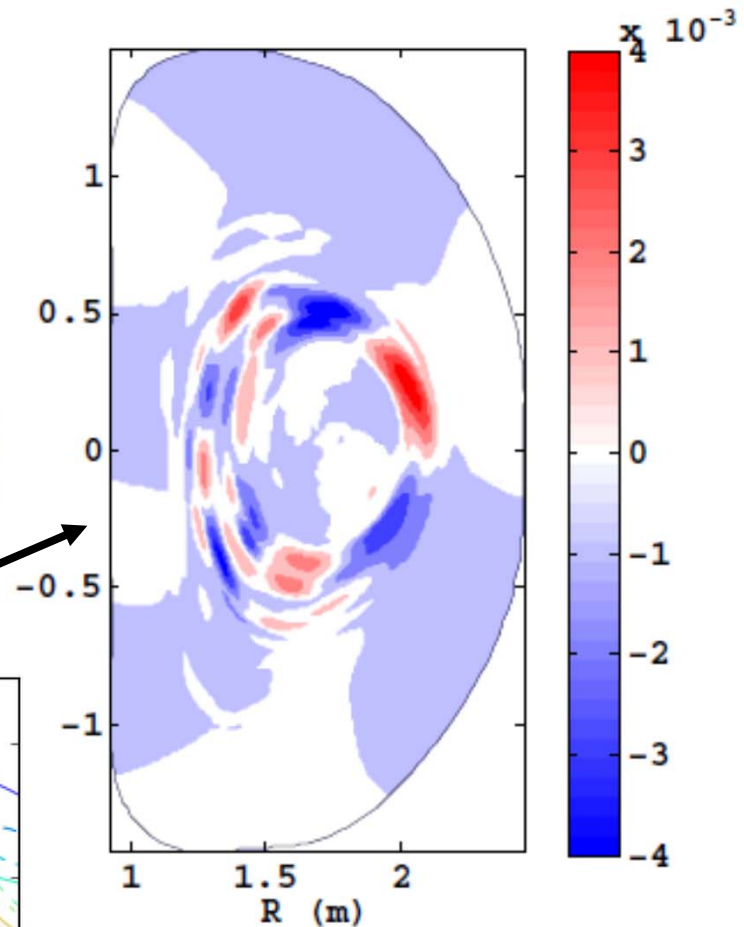
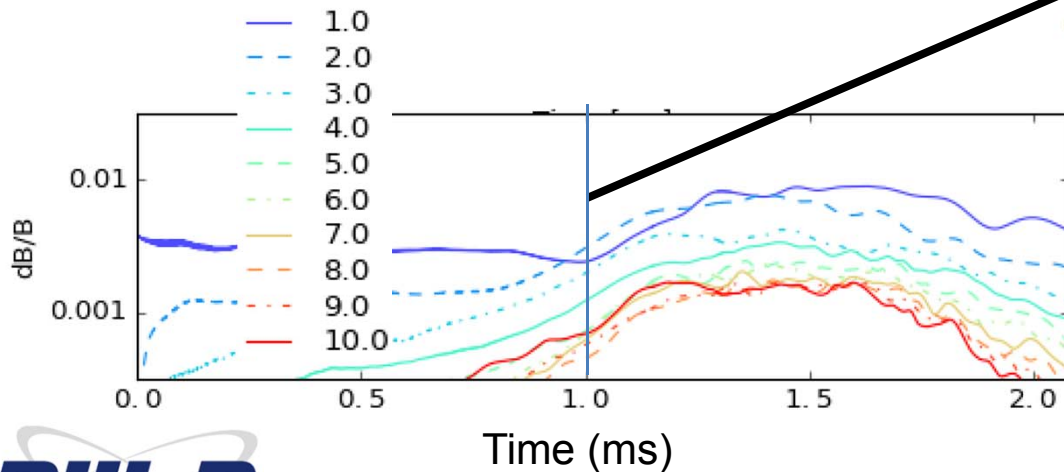


With 0-phase, impurity plume breaks up into multiple branches, begins to spread more rapidly



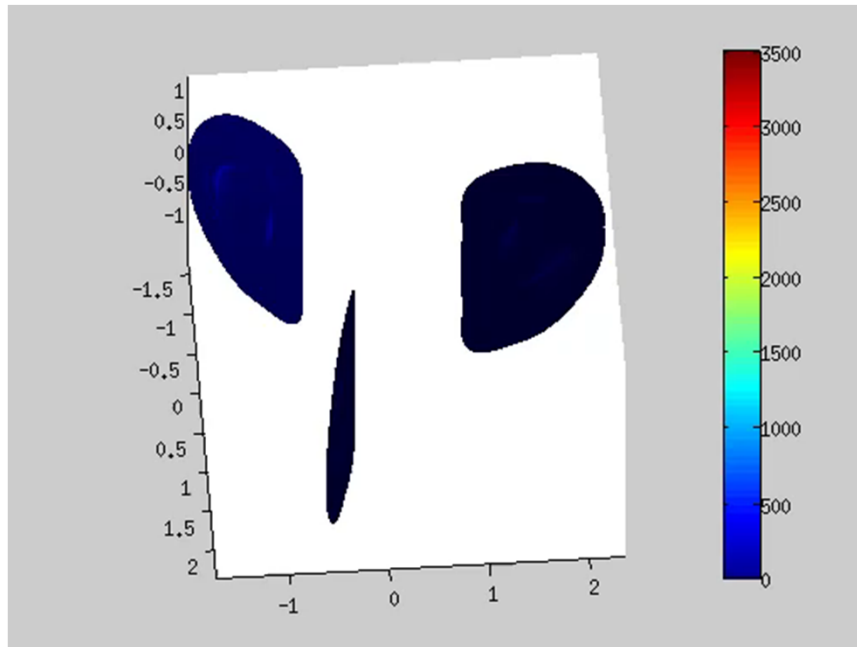
Change in impurity spreading coincident with appearance of 4/2 harmonic of 2/1

- $V_{ind} \approx 5 \text{ km/s}$ (at $t = 1.0 \text{ ms}$)
- O^{5+} $\text{I} \approx 2.4 \times 10^{-3}$ (at $t = 1.0 \text{ ms}$)
- $E_{ind} \approx 10 \text{ kV}$ (at $t = 1.0 \text{ ms}$)



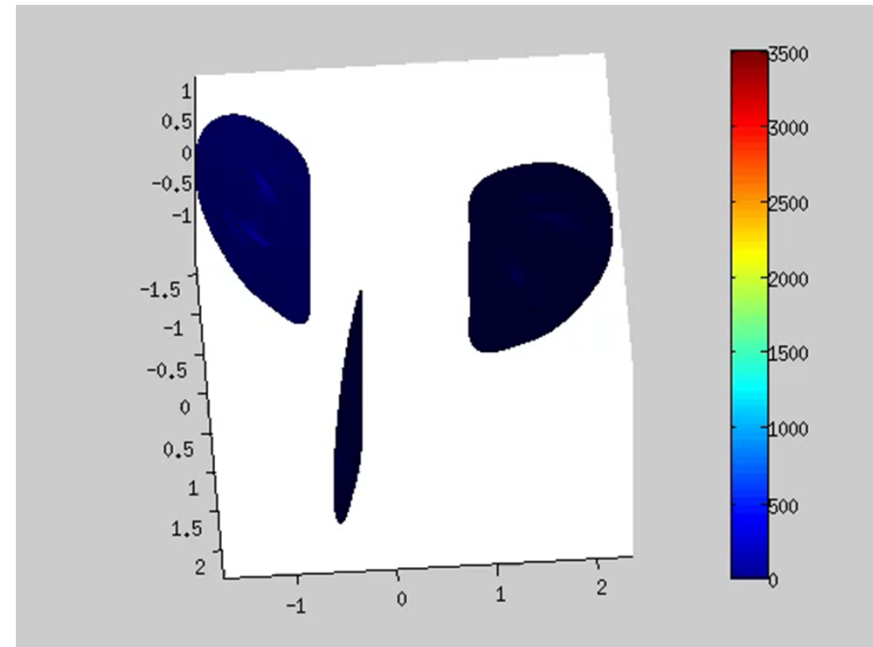
Changes in cooling near the 2/1 island are also evident when n=2 mode appears

180-phase, large island



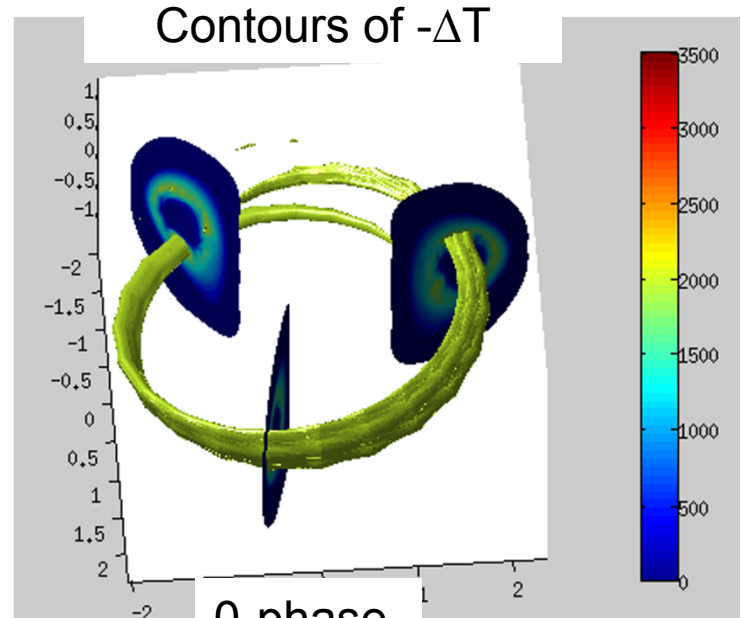
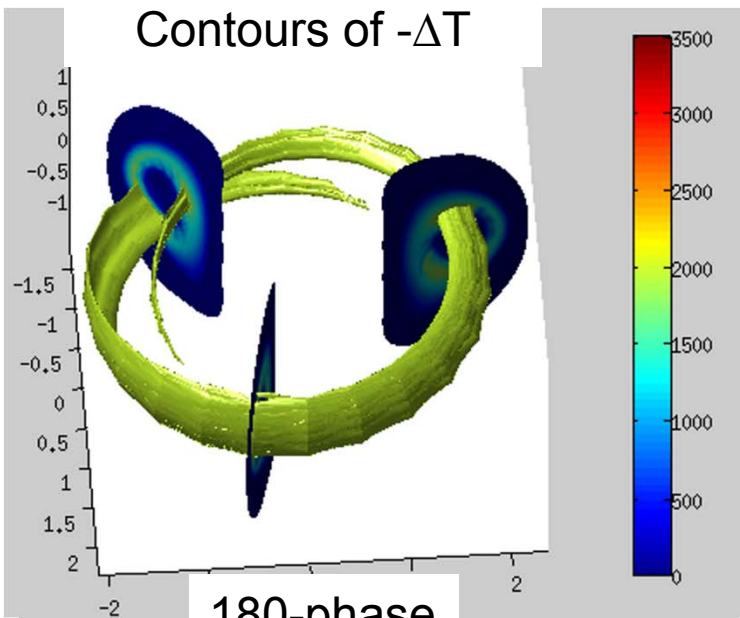
Contours of $-\Delta T$

0-phase, large island

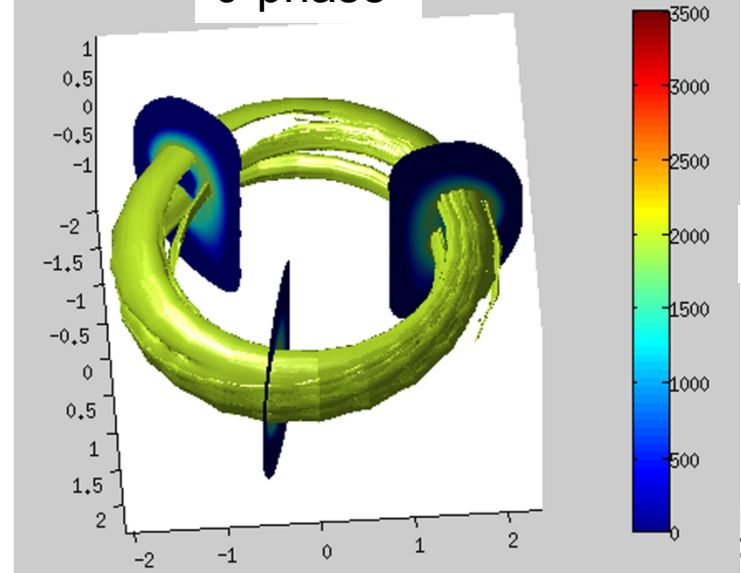
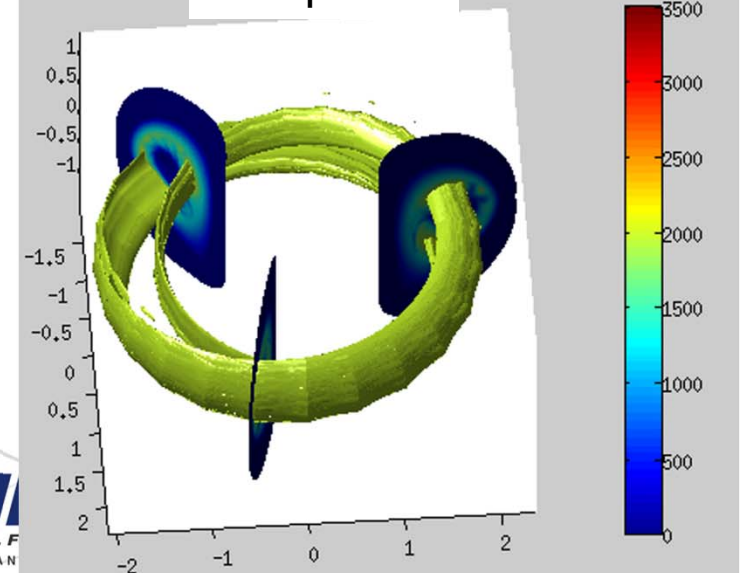


Contours of $-\Delta T$

Changes in cooling near the 2/1 island are also evident when n=2 mode appears

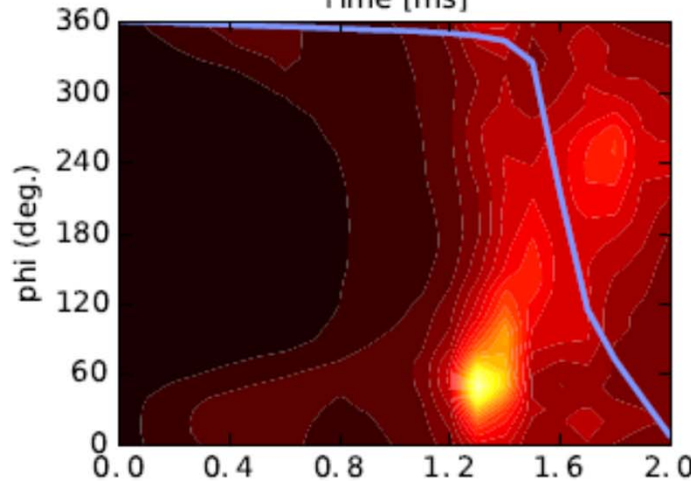
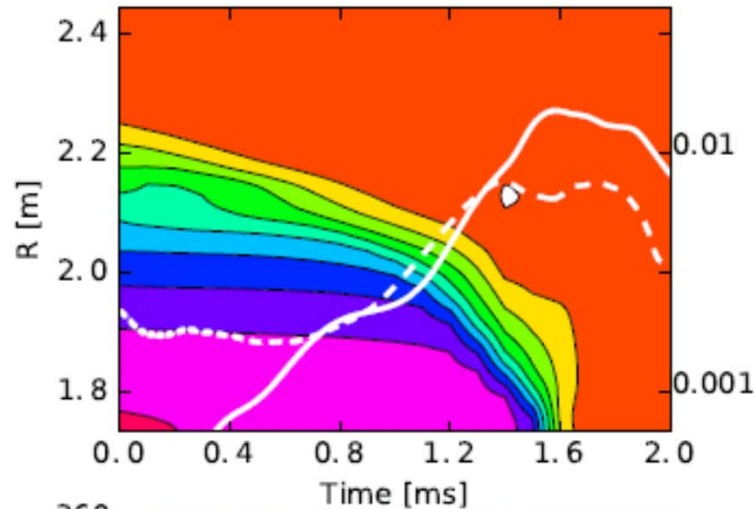
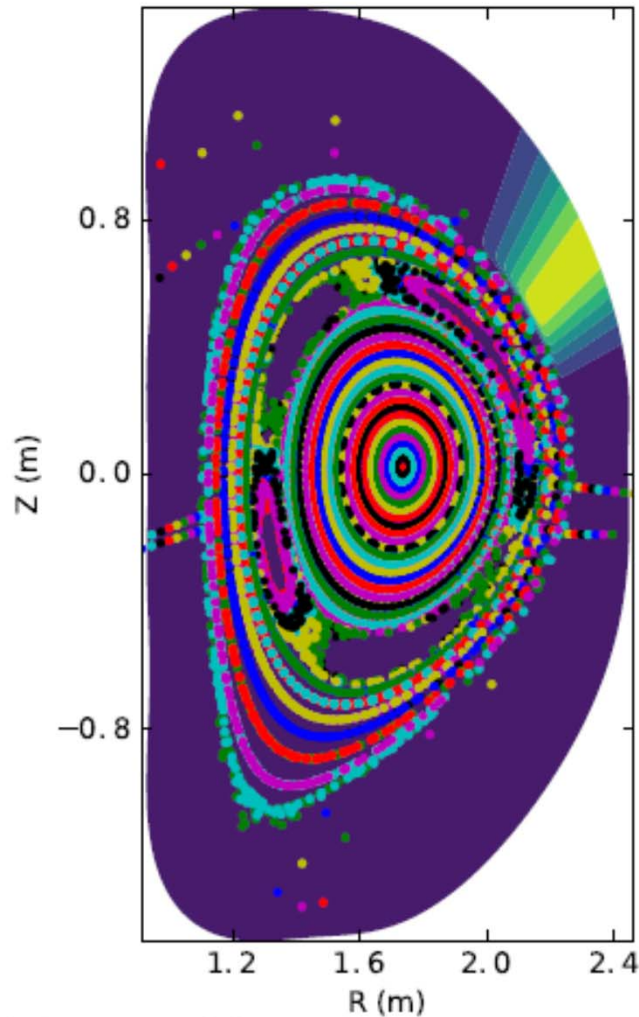


1.1 ms



1.2 ms

Direct imposition of 4/2 island can force 180-phase to behave like 0-phase case

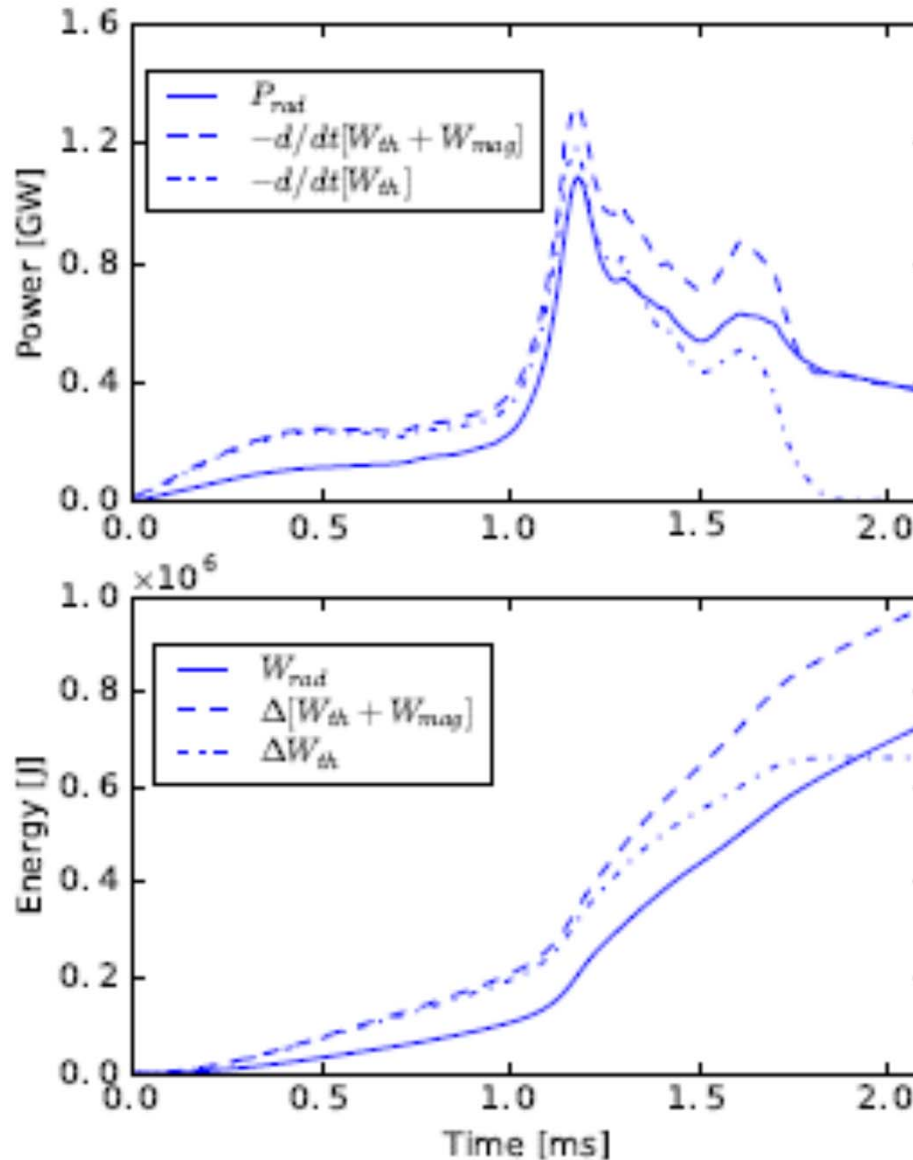


- $V_{\text{p}} \approx 10^8 \text{ m/s}$
 $725 \text{ m} \approx 10^8 \text{ m/s} \times 7.25 \times 10^{-6} \text{ s}$
 $524 \text{ m} \approx 10^8 \text{ m/s} \times 5.24 \times 10^{-6} \text{ s}$
 $\text{frp} \approx 10^8 \text{ m/s} \times 10^{-6} \text{ s}$
 $\text{skd} \approx 10^8 \text{ m/s} \times 10^{-6} \text{ s}$
 $\text{dw} \approx 10^8 \text{ m/s} \times 10^{-6} \text{ s}$
 log
- $D_{\text{w}} \approx 4 \times 10^{-4} \text{ m}^2/\text{s}$
 $\text{frp} \approx 10^8 \text{ m/s} \times 10^{-6} \text{ s}$
 $\text{dp} \approx 10^8 \text{ m/s} \times 10^{-6} \text{ s}$
 $\text{hy} \approx 10^8 \text{ m/s} \times 10^{-6} \text{ s}$
 $\text{vp} \approx 10^8 \text{ m/s} \times 10^{-6} \text{ s}$
 fd
- $I_{\text{d}} \approx 10^8 \text{ A}$
 $\text{io} \approx 10^8 \text{ A} \times 10^{-6} \text{ s}$
 $\text{skd} \approx 10^8 \text{ A} \times 10^{-6} \text{ s}$
 $\text{vs} \approx 10^8 \text{ A} \times 10^{-6} \text{ s}$
 pr

PART 3: Consequences for radiated energy fraction and toroidal peaking factor

Conducted energy fraction defined by total energy lost minus radiated energy

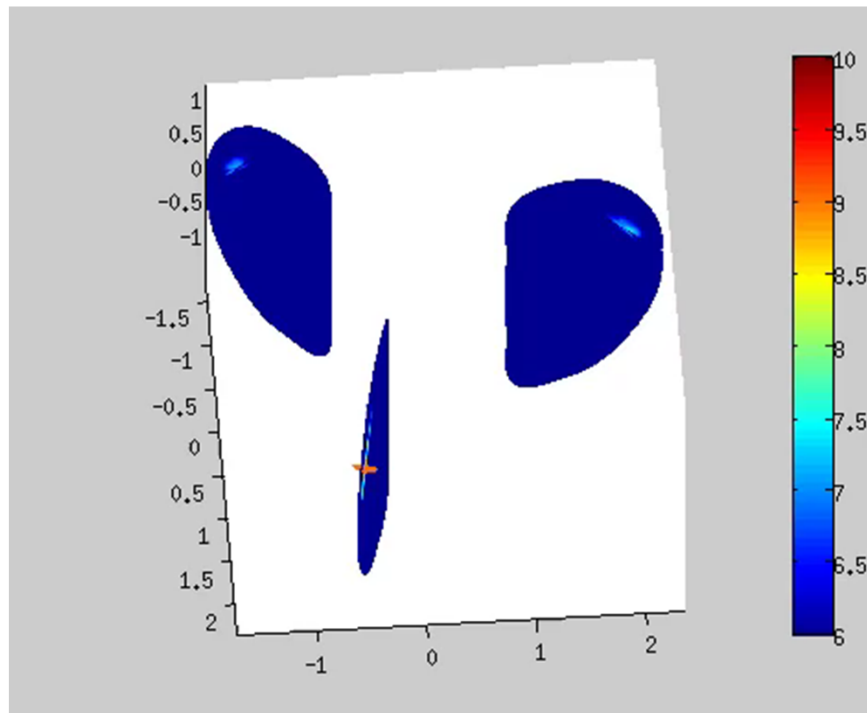
- Qhdu#hahq#huj#
arw#v#k#hup#d#
hohuj#k#s#r#k#h#
udg#b#w#g#r#z#h#
shdn
- Divu#k#h#shdn#
oujh#u#d#w#r#g#r#
arw#h#q#huj#h#v#
p#d#j#q#w#f#433#(#
divu#h#v#r#y#h#u#
- Divu#k#h#h#v#
S_{udg}@GZ 2gwdv#
Rkp If khdw#g#j#
udg#b#w#g#e#d#o#l#f#h#



- Z_{udg} 2Z_{wk} ghshogv#
vhqv#v#h#q#r#z#
hgg#r#h#v#k#r#v#h#q#
 - Ip srudq#x#d#q#w#h#
l#h#q#huj#f#r#g#g#f#w#g#
w#k#h#g#l#y#h#w#r#u#
 - Ghibh#f#r#g#g#f#w#g#
hohuj#h#u#d#w#r#g#
- i@+| Z_{wr} Z_{udg} 2Z_{wk}

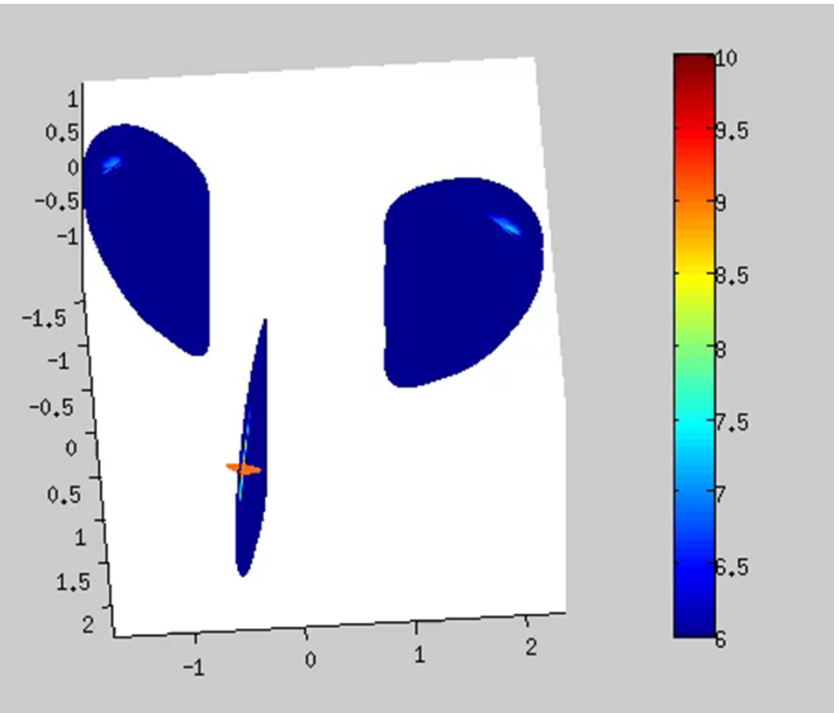
0-phase case has more uniform radiated power during most of the TQ

180-phase, large island



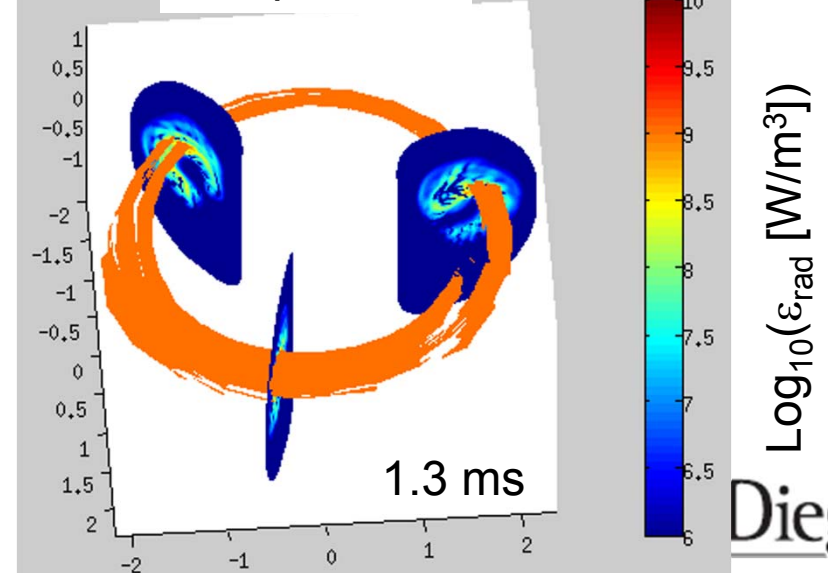
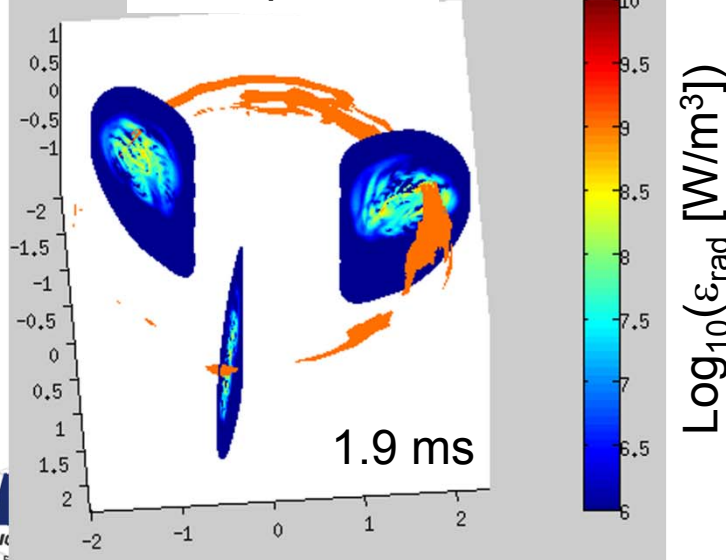
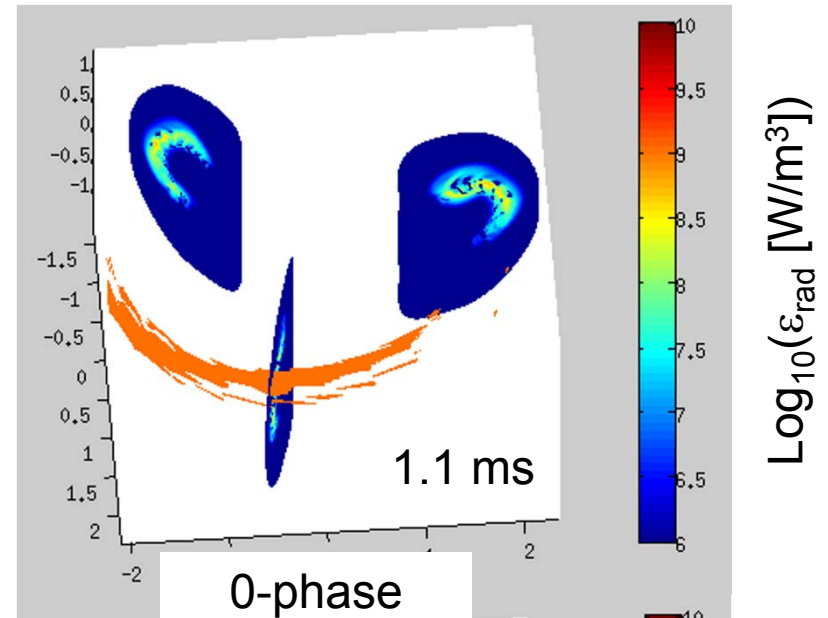
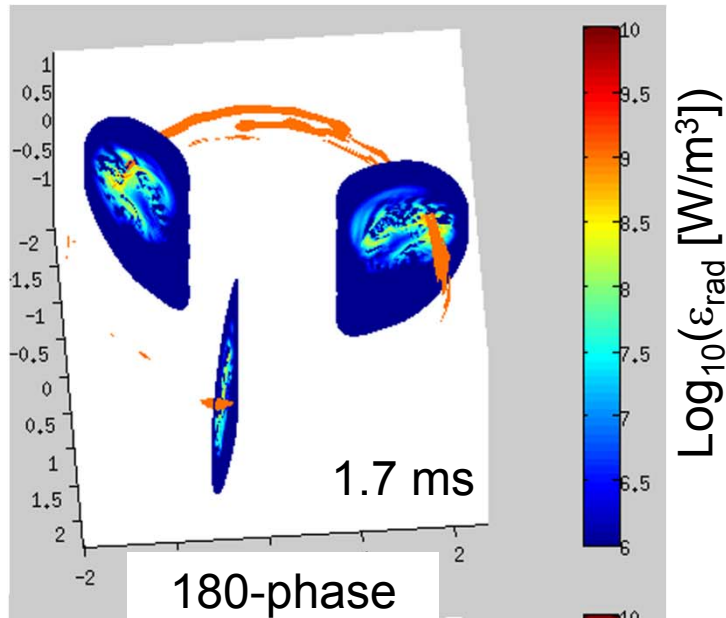
Emissivity contours

0-phase, large island



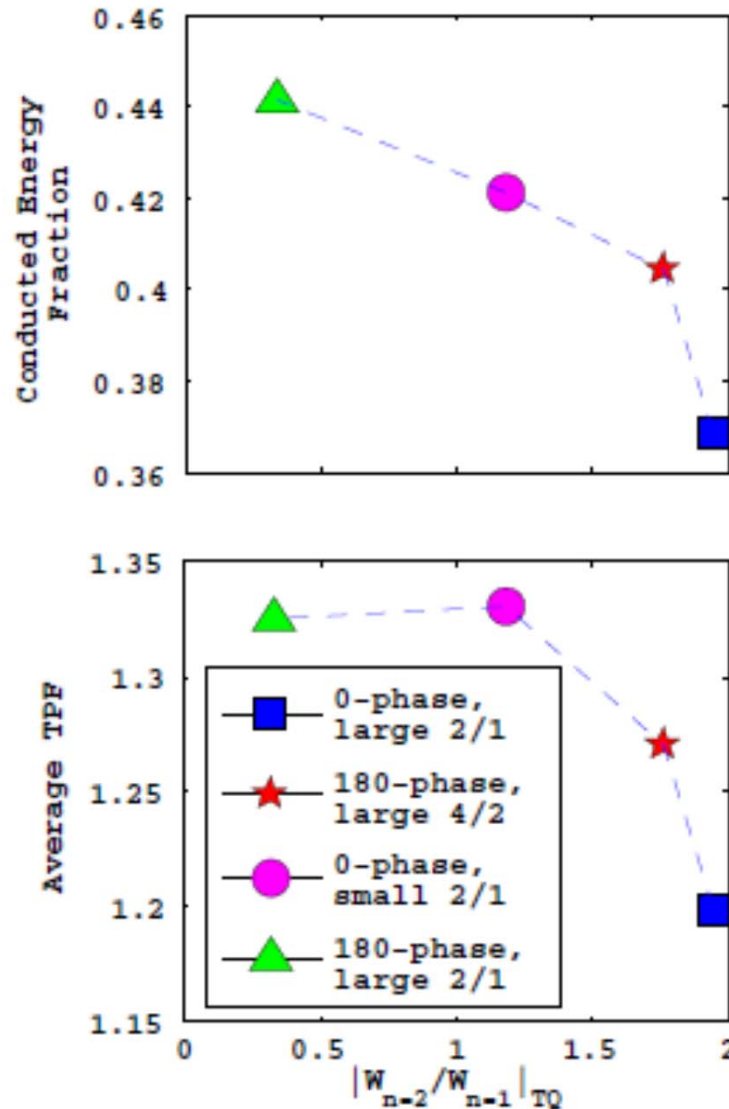
Emissivity contours

0-phase case has more uniform radiated power during most of the TQ



Better mitigation when 4/2 mode is present

- Frqgxfwng#hghj|#
iudfwirg#bg#dg bwrq##
wru rbgd#hdn bjr#
idfwr#ru#rxu#
vlp xodwlrqvU wuhh#
z lk\$24#vologv#bg#
rqh# lk#725#vologv
- Erwk#xdqwlhv#
sawhg#huxv#kh#
pd{p xp #dwr#i#kh#
q@5#r#q@4#p sdwgh#
gxulgr#kh#I#skdvh



- Erwk#xdqwlhv#
lp suryh#ungxfh,#v#
wh#hnowyn#p sdwgh#
r#kh#q@5#hfrp hv#
oljhu
- Vsrqwdqhrxvq#
jurz bjr#u#ruled#
lp srvhg#q@5#p rgh#v#
ehqhilfbdwr#
p lwdwlrq# hwilfv

Conclusions

- Magnetic topology plays a large role in determining impurity parallel transport
 - The presence of large islands affects the heat conduction and spreading of impurities at the rational surface
 - The break-up of the islands into smaller island chains enhances impurity spreading, and reduces average toroidal peaking and the conducted energy fraction
- Evolution of magnetic topology is determined by combination of gas jet(s), pre-existing MHD, (and applied fields)
 - For a single gas jet, the appearance of the $n=2$ harmonic occurs only for some island phases.
 - A deliberately imposed $4/2$ island produces a similar radiation pattern to the case with a spontaneously growing $4/2$ mode

Future work: How do these results compare with DIII-D experiments? What about multiple jets? Higher-n harmonics?